

Large-scale flow in competing-interaction systems

A. R. Bishop, S. Marianer,* and L. M. Floria[†]

Los Alamos National Laboratory, Los Alamos, New Mexico 87545

(Received 5 September 1989)

We study the dynamics of large-scale flow in a system with several competing length scales. This system, when driven, is characterized by critically metastable states. When the driving force is lowered, these states “melt” via nucleation of a low density of slowly moving defects, which control and relate the long-time, long-distance behaviors. We demonstrate these properties with a one-dimensional lattice-dynamics model for twinning in elastic materials, including (a) a periodic substrate potential, (b) a nonconvex nearest-neighbor spring potential, and (c) a harmonic next-nearest-neighbor spring potential. This system exhibits a rich spectrum of superlattice ground states. Large-scale driving, obtained by adding a constant force and damping to the equations of motion, shows four distinct regimes: (i) At high forces a metastable inhomogeneously modulated configuration moves rigidly with a velocity given by the ratio of force to damping; (ii) as the force decreases the rigidity is lost via local nucleation of soliton defects (in the double well) and fluctuations of the velocities increase; (iii) for even lower forces the configuration ceases to translate, and the dynamics is controlled by nucleation of (sine-Gordon-like) kink-antikink pairs in the substrate; and finally (iv) at a sufficiently low force a metastable configuration, consisting of a random array of solitons (in the double-well potential), is pinned. We also observe strong hysteretic behavior at the transitions.

Physical systems with competing interactions that have incommensurate length scales have become a subject of considerable interest because they can lead both to modulated ground states and to unusual excitations and dynamics. Examples of such systems are: random field magnets, pinned charge-density waves and spin glasses. While most of the theoretical studies have been limited to cases where the interparticle interactions are convex, there have been recent studies of the influence of *nonconvexity* on the ground states and on the order of the phase transitions between them.¹⁻⁶ The phase diagram obtained in these studies consists of various modulated phases with combinations of first- and second-order transitions. In previous studies⁴⁻⁶ we considered a specific

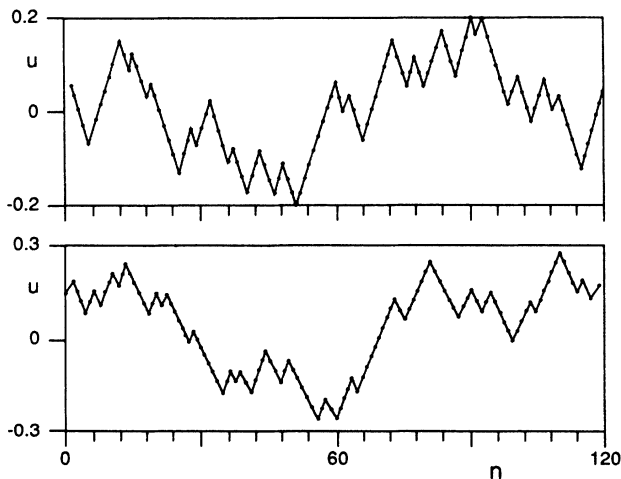


FIG. 1. Typical configurations obtained in the high-force regime. The exact shapes of the configurations are determined by initial conditions and the values of the parameters are given in the text.

model in this nonconvexity class [Eq. (1)], and studied the influence of the nonconvexity on its ground states and excitations. In particular, we obtained the phase diagram and the order of the phase transitions between various superlattice ground states as the parameters are varied. We were also able to show⁴ that the nature of excitations defined with respect to these modulated ground states is changed from extended kinks to narrow, pinned ones as the interparticle interactions change from convex to concave character, respectively.

In what follows we report *transport* results that we have obtained in the presence of dc driving. We show that this driving results in critically metastable states which melt via nucleation of a low density of slowly moving defects that control and relate the long-time, long-distance behaviors. We believe this is typical of the dy-

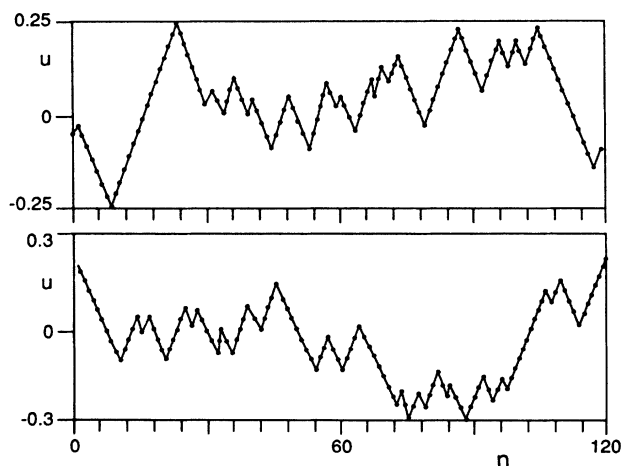


FIG. 2. The same as Fig. 1 but for driving without a substrate.

namics of complex patterns (resulting from competing interactions); namely transport is controlled by defects generated with respect to those patterns: similar concepts have also been discussed in recent literature on $1/f$ noise⁷ and in turbulent flows.⁸

We use here an extension of the familiar Frenkel-Kontorova model in which we introduce double-well interparticle springs, and where we model the strain gradients by next-nearest-neighbor interactions. The Hamiltonian for the system is given by

$$H = \sum_n \dot{u}_n^2/2 + \alpha(u_{n+1} - u_n)^4 - \beta(u_{n+1} - u_n)^2 + (\gamma/2)(u_{n+1} - 2u_n + u_{n-1})^2 - \cos u_n. \quad (1)$$

This model may be useful in the description of twinning in martensitic materials, as was pointed out by Barsch, Horowitz, and Krumhansl.^{9,10} In this case the substrate potential ($\cos u_n$) models the parent phase and the other terms are the expansion of the elastic free energy as a function of the discretized strain and strain gradients. Note that the second-neighbor springs are important for the superlattice ground states to appear—with $\gamma=0$ only dimerized and uniform ground states occur.⁴ Similarly, the appearance of critically metastable states in our one-dimensional driven system (in the following) requires the additional complexity allowed by this expansion of phase space (i.e., $\gamma \neq 0$). Throughout this work we fix the value

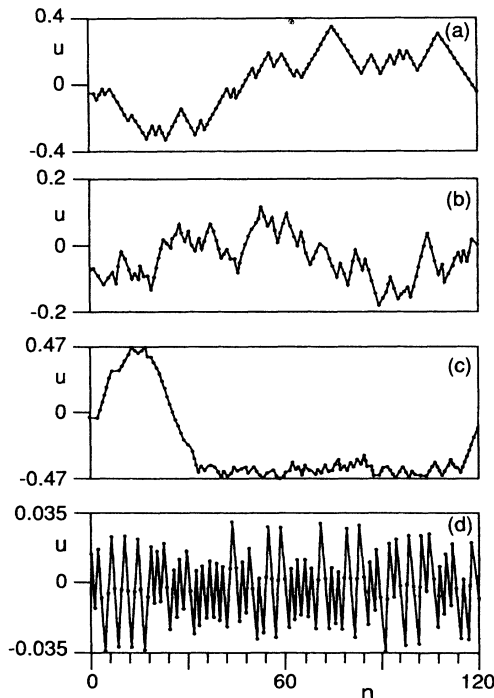


FIG. 3. (a) The rigid inhomogeneously modulated configuration obtained in the high-force regime. (b) Lowering the force, localized phonons are excited and the rigidity is lost. (c) For even lower force the configuration evolves by forming sine-Gordon-like kink-antikink pairs in the substrate potential. (d) The final metastable configuration into which the system relaxes. The relative displacements on the vertical axes are in units of 2π (the period of the substrate). Note the different scales in the figures.

of α to be $\alpha=20$. This choice is made in order to restrict the positions of the minima of the double well, $\pm l_0 = \sqrt{\beta/2\alpha}$, to be small relative to the parent phase lattice constant (2π in the units we use here). Indeed typical values of the change in the lattice constant in tetragonal to orthorhombic transitions is usually found to be of the order of 1–3%.

To study the dynamics of large-scale driving we add a constant force F as well as damping $\epsilon\dot{u}$ to the equations of motion obtained from the Hamiltonian (1). The modified equations are then given by:

$$\begin{aligned} \ddot{u}_n = & 4\alpha[(u_{n+1} - u_n)^3 - (u_n - u_{n-1})^3] \\ & - 2\beta(u_{n+1} - 2u_n + u_{n-1}) \\ & - \gamma(u_{n+2} - 4u_{n+1} + 6u_n - 4u_{n-1} + u_{n-2}) \\ & - \sin u_n + F - \epsilon\dot{u}_n. \end{aligned} \quad (2)$$

Our numerical simulations were made with the following additional parameter values: $\beta=1.5$, $\gamma=0.1$, and $\epsilon=0.01$, (i.e., the motion of the particles is underdamped). This point in the parameter space belongs to the dimerized phase in the ground-state phase diagram^{5,6} but it is relatively close to the first-order transition line between the dimerized and quadrimerized ground states. As the force is varied we observe four distinct regimes.

(i) A high-force regime in which an inhomogeneously modulated configuration moves *rigidly* with a velocity given by: $v = F/\epsilon$. Typical examples of such configurations are shown in Fig. 1, and we observe that these consist of long segments where the interparticle distances are determined by the minima of the double

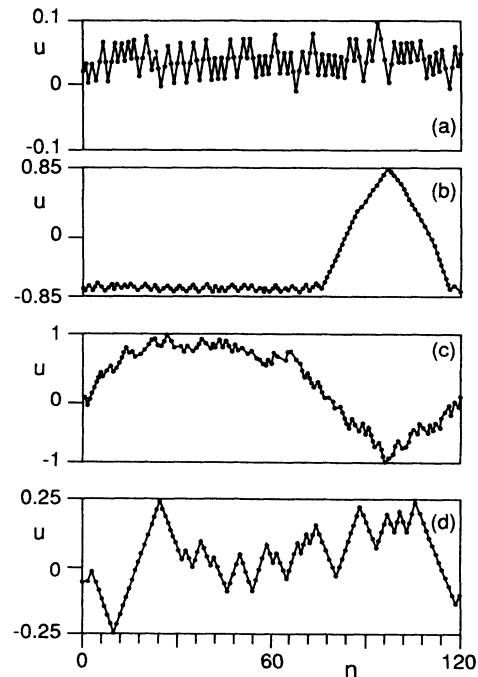


FIG. 4. The same configurations obtained in Fig. 3 but for the case of increasing the force (and thus in reversed order). The relative displacements on the vertical axes are in units of 2π (the period of the substrate). Note the different scales in the figures.

well with kinks in the double-well potential marking the change from short ($u_{n+1} - u_n = -l_0$) to long ($u_{n+1} - u_n = +l_0$) interparticle springs. The distribution of the distances between such kinks is determined by the value of γ , whereas their exact locations depend on the initial conditions. The rigid motion of the chain in this regime suggests (as for the strongly driven sine-Gordon chain¹¹) that the influence of the substrate on the particles is negligible and the details of the configuration are determined by the interparticle coupling constants (i.e., α , β , and γ). To demonstrate that this is indeed the case we repeated our numerical simulation with the substrate potential set to zero. The results of this simulation are shown in Fig. 2 and we indeed observe rigid motion of configurations similar to those obtained in Fig. 1. There is, however, an important distinction between these two cases (i.e., with and without a substrate), namely the value of the force needed to obtain them. While there is a lower bound on the force (depending on whether we are increasing or decreasing the force because of a hysteric effect that we discuss in the following) when the substrate is present, the lower bound is zero for driving the free chain.

(ii) As the force decreases (and thus also the velocity F/ϵ) a value is reached beyond which the rigidity is lost and “localized phonons” are excited on the moving chain which saturate (in the nonlinearity) into kink defects in the double-well springs. This happens at a velocity given by $v \approx 5$ and thus a force $F = v\epsilon \approx 0.05$, for the values of the parameters that we have used. An example is shown in Fig. 3(b).

(iii) For an even lower force, the structure ceases to translate and evolves alternatively by forming kink-antikink pairs in the substrate [see Fig. 3(c)].

(iv) Finally a metastable configuration forms which consists of a random array of solitons in the double well [e.g., a mixture of dimers and quadromers as shown in Fig. 3(d)].

This process can be reversed starting from a metastable configuration obtained for the case $F=0$ and increasing the force. The results are shown in Fig. 4 and we see that the system evolves in reverse order through the same states that were obtained when the force was decreased, viz., the metastable dimer-quadromer mixture melts by forming kink-antikink pairs in the substrate [Fig. 4(b)] and these evolve, by creation of high-frequency localized phonons, into the inhomogeneously modulated rigid structure [Figs. 4(c) and 4(d)]. A striking result of these simulations is the observation of a strong hysteresis as the force is varied. While the threshold for formation of the modulated rigid structure when the force is increased is $F \approx 1$, the condition for losing rigidity when the force is lowered is much smaller ($F \approx 0.05$).

This hysteric behavior can be understood as follows. Coming from the low-force region (Fig. 4) we need a depinning force $F \approx 1$, where 1 is the strength of the substrate, in order to overcome the barrier for creating the sine-Gordon kink-antikink pairs shown in Fig. 4(b) and to melt the initial metastable structure of solitons in the double well [Fig. 4(a)]. On the other hand, coming from the high-force regime where the configuration moves rig-

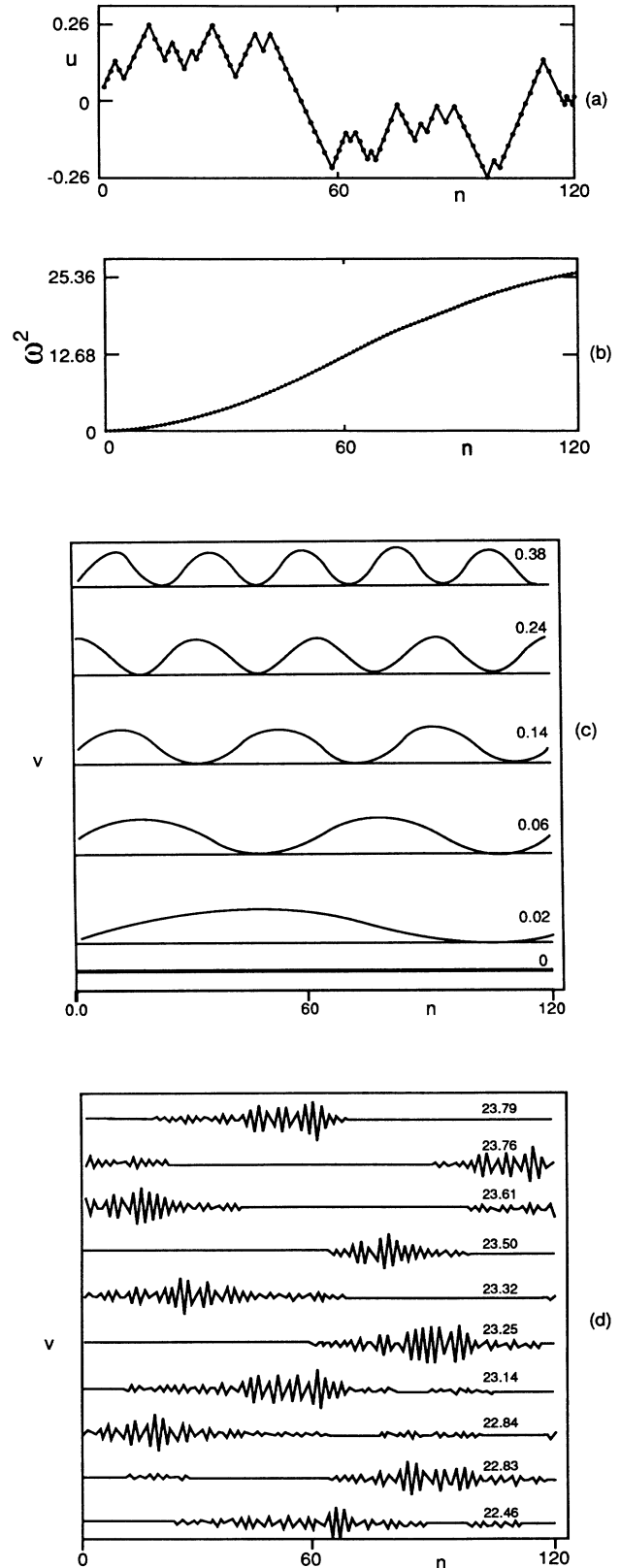


FIG. 5. (a) The inhomogeneously modulated configuration whose linear stability is analyzed. (b) The spectrum of ω^2 . (c) The lowest-frequency modes (the numbers denote the corresponding values of ω^2). (d) The highest-frequency modes.

idly with a velocity $v = F/\epsilon$ this configuration will be stable until the substrate can excite localized phonons which will destroy the rigidity and eventually melt it. The condition for this to happen is that the velocity should be low enough as we now explain.

When the chain is moving rigidly in the substrate the latter exerts a force on it given by $F_{\text{substrate}} = -\sin u = -\sin(vt)$ where v is the velocity of the chain. This acts like a periodic driving with periodicity $\omega = v$ and can thus excite phonons with frequency $\omega_{ph} = v$. We have performed a linear stability analysis on the configurations (without the substrate) and obtained the following results (see Fig. 5): The low-frequency phonons are extended (almost harmonic ones) with the lowest frequency being $\omega = 0$ for a rigid translation, while the highest-frequency ones are those localized on the *longest* segments of the chain and the highest frequency is thus given by

$$\omega_{\text{max}} = \sqrt{16(\beta + \gamma)}. \quad (3)$$

This result is exact for an infinite chain and substituting the values for β and γ we indeed obtain $v = \omega_{\text{max}} = 5$ and thus a force $F = 0.05$. For finite lengths we obtain (to lowest order in $1/L$):

$$\omega_{\text{max}}^2 = 16(\beta + \gamma) - (\pi/L)^2(8\gamma + 4\beta). \quad (4)$$

This last result is obtained as follows. The deviations v_n about the static solution $u_n = nl_0$ of Eq. (2) (with the substrate, damping and driving forces turned off) obey the following equations (to linear order):

$$\begin{aligned} \ddot{v}_n = & -4\beta(v_{n+1} - 2v_n + v_{n-1}) \\ & -\gamma(v_{n+2} - 4v_{n+1} + 6v_n - 4v_{n-1} + v_{n-2}). \end{aligned}$$

Substituting a solution $v_n = V \sin kn \sin \omega t$, we get:

$$\omega^2 = 16(\beta + \gamma) \sin^2(k/2) - 4\gamma \sin^2 k.$$

Substituting in this equation the value $k = \pi - \pi/L$ which is the largest wave vector for a chain of length L we obtain Eq. (4). Thus we see here how the spatial configuration can influence the temporal behavior via the phonon spectrum. Specifically, the distribution of kinks excited (in the double wells) is determined by the distribution of length scales in the rigidly rotating configuration. This behavior should be contrasted with the driven sine-Gordon chain¹¹ (i.e., harmonic springs). There the rotating state is spatially homogeneous and thus linearly unstable modes are *extended* phonons that saturate into a periodic wavetrain of “breather” modes uniformly distributed along the whole chain.

Finally it is worth mentioning that the behavior of the system and in particular the final configuration into

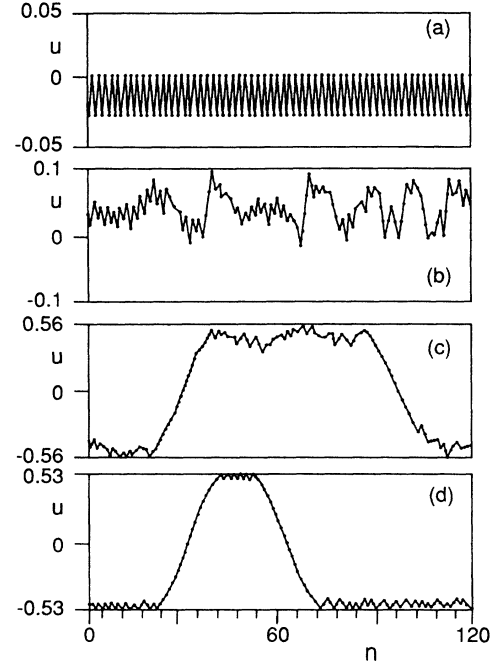


FIG. 6. The same as Fig. 4 but starting from an exact (i.e., dimerized) ground state. Here the final state is a sine-Gordon-like soliton-antisoliton pair.

which it evolves are not unique. In Fig. 6 we show a simulation in which we decreased the force in the same way as in the simulation described in Fig. 3, the only difference being that here we start with a running, purely dimerized state (the exact ground state of the system for the values of the parameters used). We see [Fig. 6(d)] that in this case the sine-Gordon soliton-antisoliton pair is stabilized by dimers and quadromers that decorate it (i.e., there is an effective repulsive interaction), and does not evolve into the random array of dimers and quadromers that is found for “arbitrary” initial conditions.

To summarize we have presented here a study of large scale dynamics in a system with competing interactions. We have shown two main mechanisms for transition from low-energy metastable states to high energy running inhomogeneously modulated configurations. Namely, a soliton-driven transition accompanied by a localized phonon driven one. We also found that these transitions are characterized by strongly hysteretic behavior. We found in the low-force regime that sine-Gordon-like soliton configurations can be stabilized by dimerized patterns.

An intriguing result of our study is that critically metastable states⁷ “melt” via nucleation of a low density of slowly moving defects which control and relate the long-time, long-distance behaviors.⁸ It will be extremely interesting to test for the absence or presence of $1/f$ noise in both time *and* space.

*Present address: Theoretical Physics Institute, University of Minnesota, 116 Church Street, Minneapolis, MN 55455.

†Permanent address: Instituto de Ciencia de Materiales de Aragón, CSIC-Universidad de Zaragoza, 50009 Zaragoza, Spain.

¹S. Aubry, K. Fesser, and A. R. Bishop, J. Phys. A **18**, 3157 (1985).

²M. Marchand, K. Hood, and A. Caille, Phys. Rev. Lett. **58**, 1660 (1987).

³C. S. O. Yokoi, L. Tang, and W. Chou, Phys. Rev. B **37**, 2173

- (1988).
- ⁴S. Marianer, A. R. Bishop, and J. Pouget, in *Competing Interactions and Microstructures: Statics and Dynamics*, Vol. 27 of *Springer Proceedings in Physics*, edited by R. LeSar, A. R. Bishop, and R. H. Heffner (Springer, New York, 1988).
- ⁵S. Marianer and A. R. Bishop, *Phys. Rev. B* **37**, 9893 (1988).
- ⁶S. Marianer and L. M. Floria, *Phys. Rev. B* **38**, 12054 (1988).
- ⁷P. Bak, C. Tang, and K. Wiesenfeld, *Phys. Rev. Lett.* **59**, 381 (1987).
- ⁸H. Chaté, Ph.D. thesis, Université Pierre et Marie Curie, Paris, 1989.
- ⁹G. R. Barsch and J. A. Krumhansl, *Phys. Rev. Lett.* **53**, 1069 (1984).
- ¹⁰G. R. Barsch, B. Horowitz, and J. A. Krumhansl, *Phys. Rev. Lett.* **59**, 1251 (1987).
- ¹¹J. C. Ariyasu and A. R. Bishop, *Phys. Rev. B* **35**, 3207 (1987); see also S. Aubry and L. de Seze, *Festkörperprobleme* **XXV**, 59 (1985).